Microfluidic Affinity Profiling reveals a Broad Range of Target Affinities for Anti-SARS-CoV-2 Antibodies in Plasma of COVID-19 Survivors

Matthias M. Schneider[1,#], Marc Emmenegger[2,#], Catherine K. Xu[1,#], Itzel Condado Morales[2,#], Georg Meisl[1], Priscilla Turelli[3], Chryssa Zografou[2], Manuela R. Zimmermann[1], Beat M. Frey[4], Sebastian Fiedler[5], Viola Denninger[5], Raphaël P. B. Jacquat[1], Lidia Madrigal[2], Alison Ilsley[5], Vasilis Kosmoliaptsis[6,7], Heike Fiegler[5], Didier Trono[3], Tuomas P. J. Knowles[1,8*] , and Adriano Aguzzi[2*]

[1] Centre for Misfolding Diseases, Yusuf Hamied Department of Chemistry, University of Cambridge, Lensfield Road, Cambridge CB2 1EW, UK
[2] Institute of Neuropathology, University of Zurich, 8091 Zurich, Switzerland
[3] School of Life Sciences, École Polytechnique Fédérale de Lausanne, Lausanne, Switzerland
[4] Regional Blood Transfusion Service Zurich, Swiss Red Cross, 8952 Schlieren, Switzerland
[5] Fluidic Analytics, Unit A, The Paddocks Business Centre, Cherry Hinton Rd, Cambridge CB1 8DH, UK
[6] Department of Surgery, Addenbrooke's Hospital, University of Cambridge, Hills Road, Cambridge CB2 0QQ, UK
[7] NIHR Blood and Transplant Research Unit in Organ Donation and Transplantation, University of Cambridge, Hills Road, Cambridge CB2 0QQ, UK
[8] Cavendish Laboratory, Department of Physics, University of Cambridge, JJ Thomson Ave, Cambridge CB3 0HE, UK
[#] equal contribution
*to whom correspondence should be addressed: adriano.aguzzi@usz.ch or tpjk2@cam.ac.uk

Supplementary Information

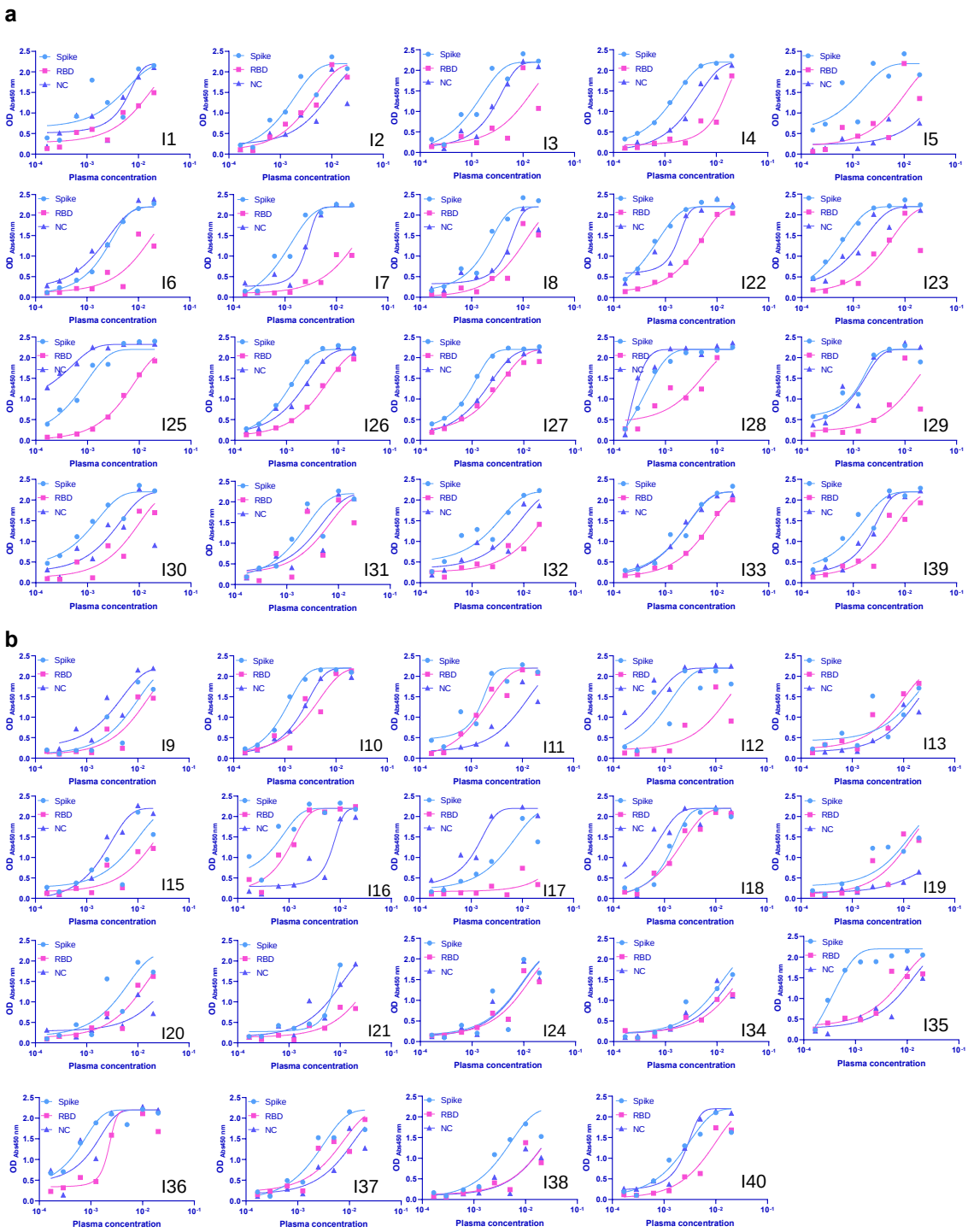

Figure S1: ELISA data for the different donors[1]. In light blue, the binding to the spike protein, in pink to the RBD and in blue triangles to NC is shown. (**a**) Convalescent individuals, (**b**) Healthy donors.

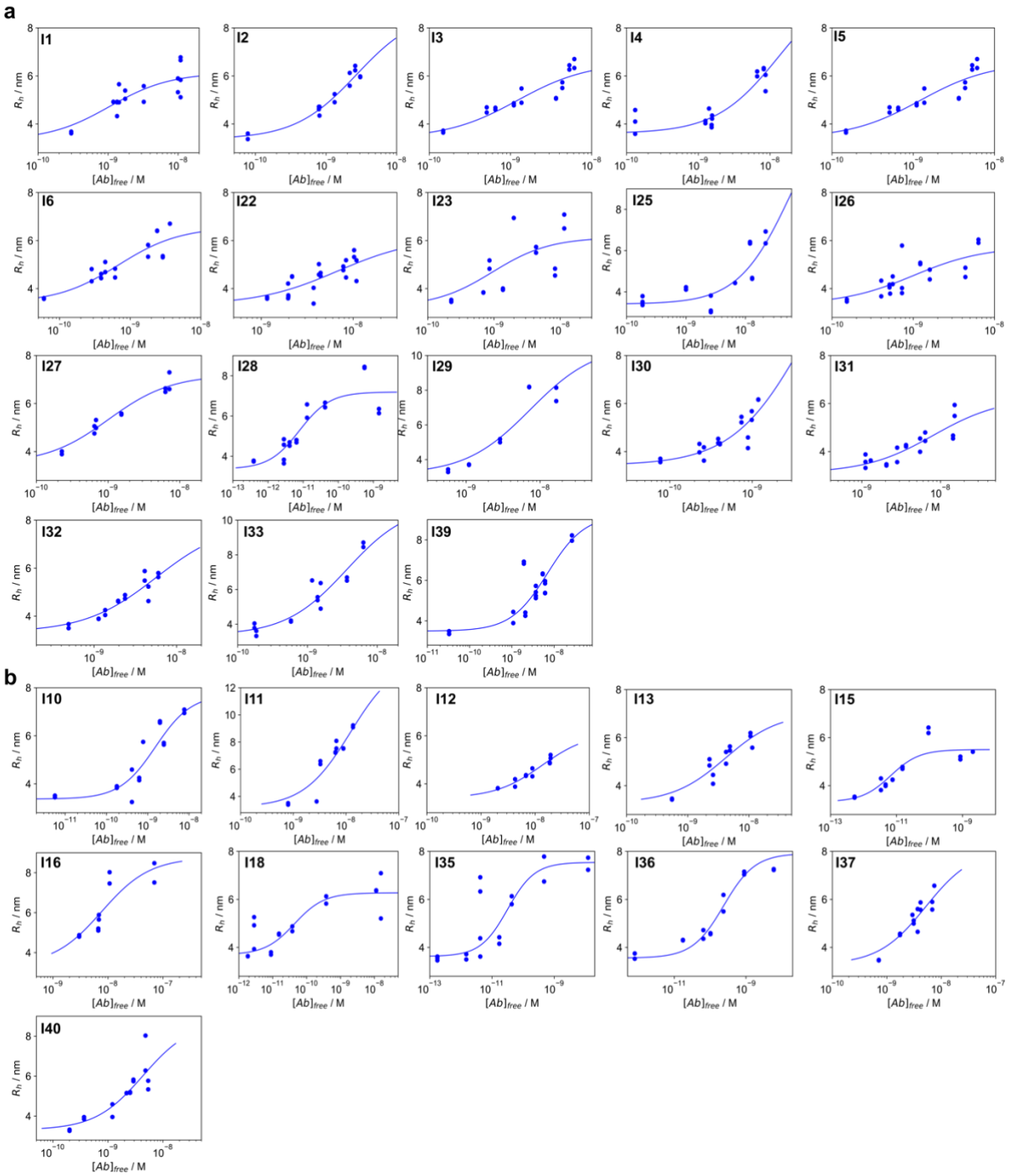

Figure S2: Binding curves for all non-hospitalised patients in Fig. 3b. (**a**) Convalescent Donors and (**b**) Healthy Donors.

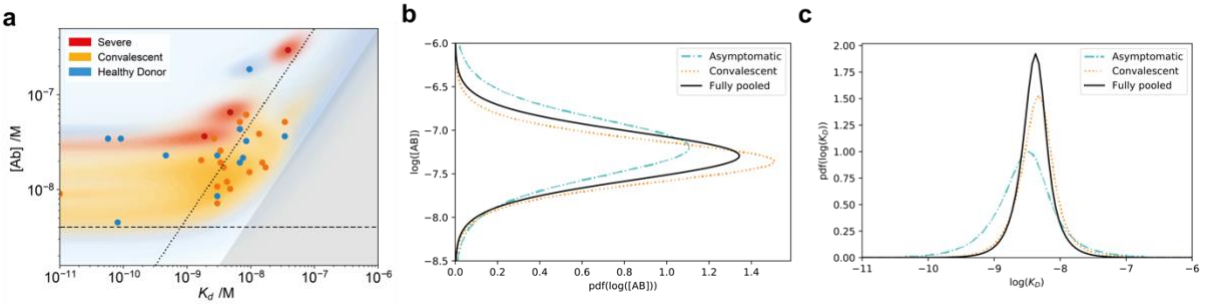

Figure S3: (**a**) Probability distributions of dissociation constants, K_d, and antibody concentrations in Figure 2B (assuming two RBD binding sites per antibody). Healthy donors (blue), PCR confirmed convalescent (orange), and severely afflicted (red) patients. Points correspond to the maximum probability values in the two-dimensional probability distribution, and coloured regions to the probability density. We do not observe significant difference in either K_d or concentration between different symptom severities. (**b-c**) To address the question whether either log(K_d) and/or log([*AB*]) differ significantly between asymptomatic and convalescent patients, we analysed the likelihoods from (a) with a partially pooled (grouped by symptoms) and fully pooled hierarchical model[2], as described in methods. (**b**) displays the posterior distribution for $\theta = \log([AB])$ and (**c**) for $\theta = \log(K_d)$. The observation that the posterior distributions for asymptomatic (dashed) and convalescent (dotted) patients in the partially pooled model are largely overlapping with one another and the posterior distribution for the fully pooled model (solid) suggests that there are no significant differences between log(K_d) and log([*AB*]) based on the symptoms experienced.

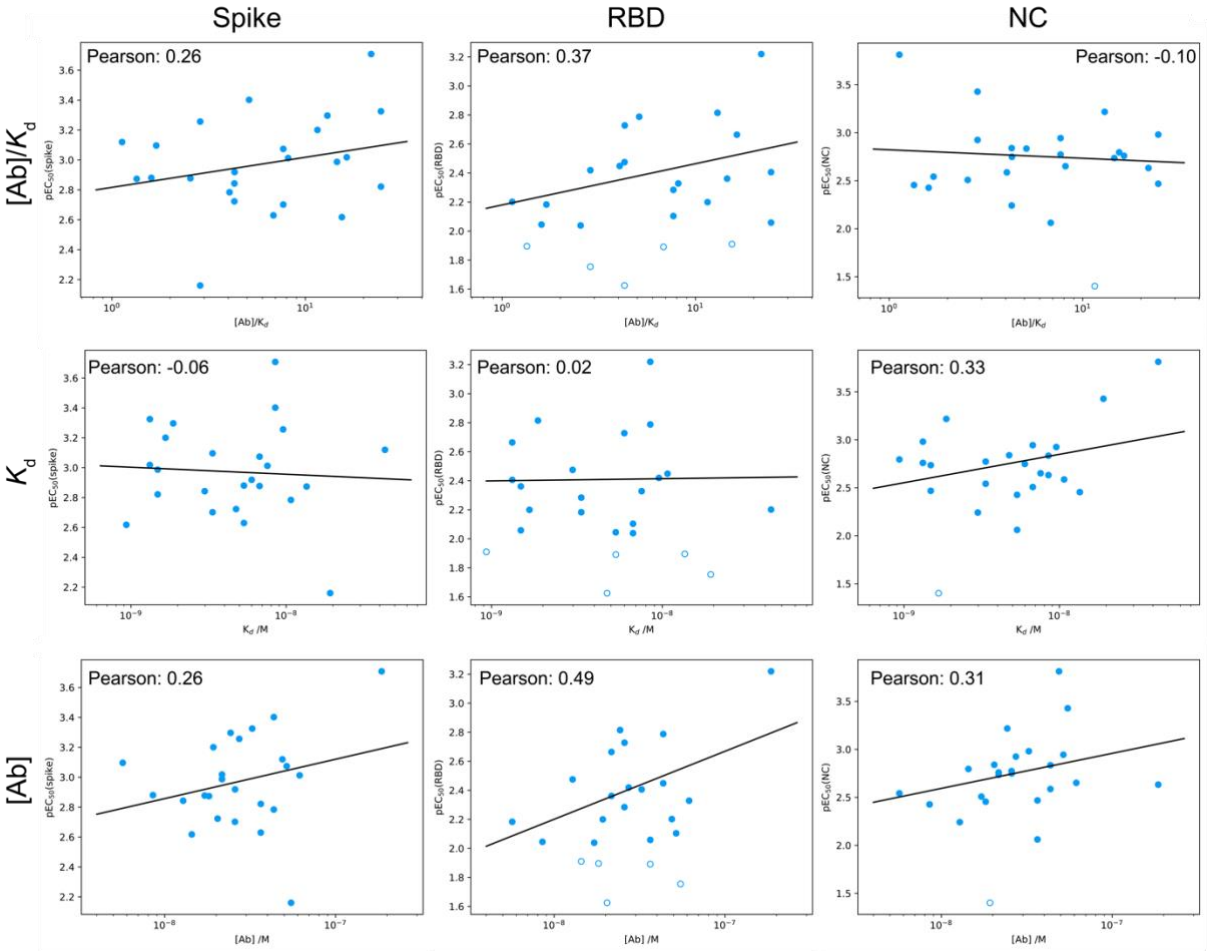

Figure S4: Comparison between ELISA (spike: left column, RBD: middle column, and nucleocapsid: right column antigens) and MAAP results for RBD binding. Plots of the pEC_{50} value are shown in comparison to the MAAP-determined ratio of antibody concentration to K_d (top row), K_d (middle row), and antibody concentration (bottom row). Only samples which yielded a peaked posterior distribution in both K_d and antibody concentration are shown, of which only those with $pEC_{50} > 2$ (filled) were used for the linear regression. Remaining data are shown as open circles. Pearson correlation coefficients are given for each plot.

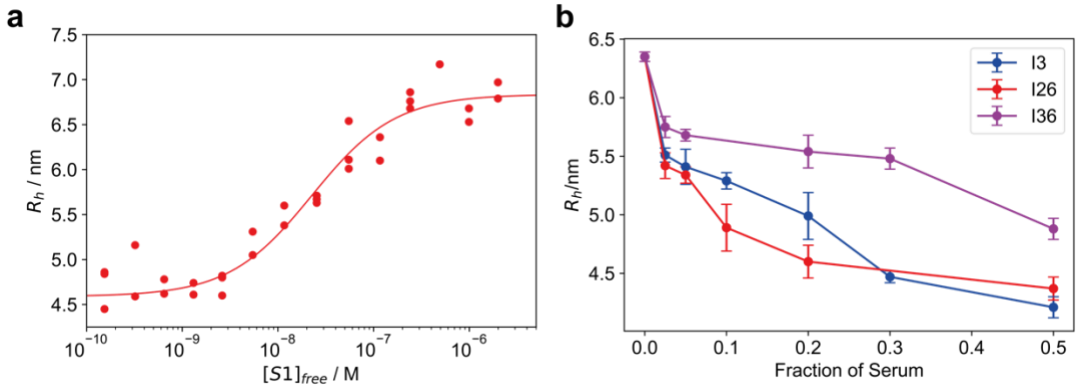

Figure S5: ACE2 competition, (**a**) Binding curve of 10 nM ACE2 against fluorescently labelled S1 protein, showing a K_d of 18 [11, 29] nM. Triplicates are shown as individual points. (**b**) Dilution series, showing concentration dependent decrease of hydrodynamic radii in three COVID-19 infected individuals in the competition assay outlined in Figure 3. Error bars are the standard deviation of triplicate measurements.

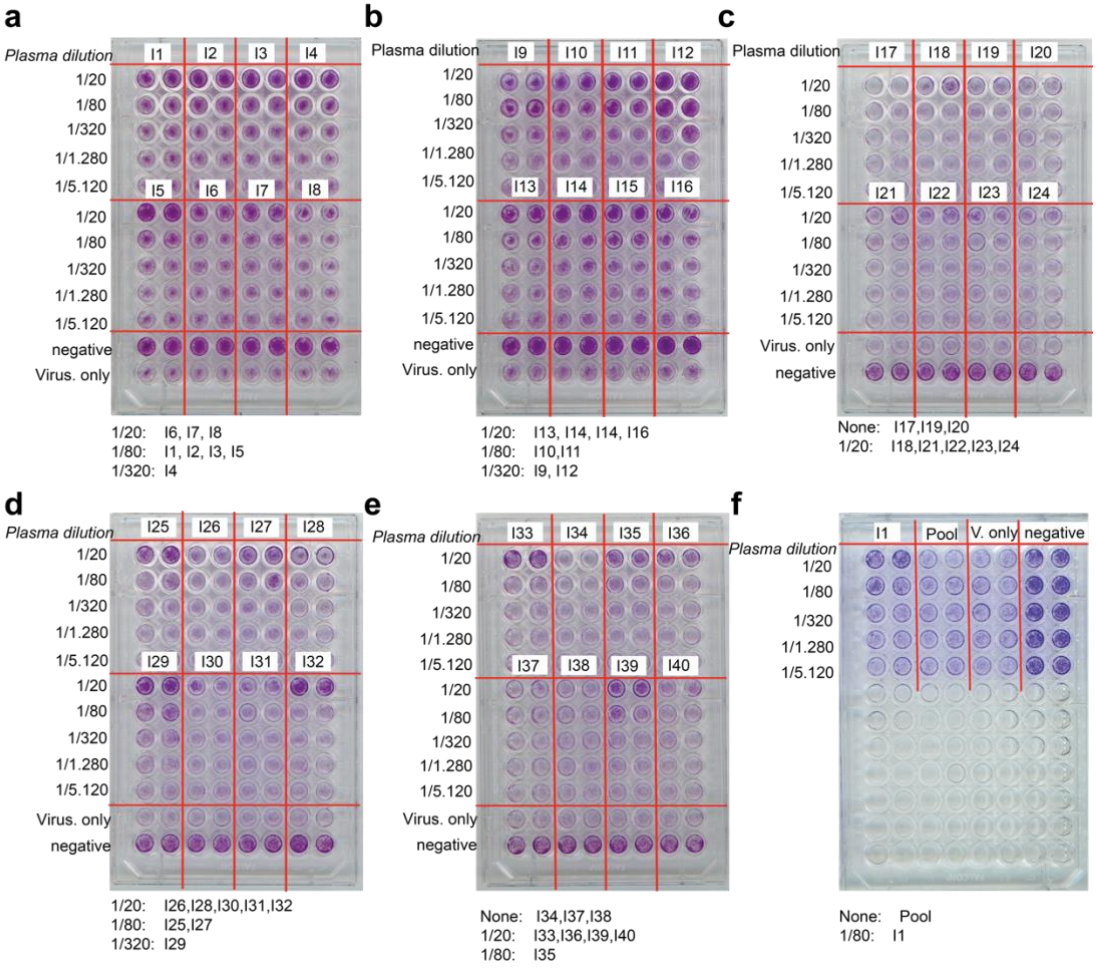

Figure S6: Cytopathic effect-based neutralisation assay. Overview over all plates with the respective interpretation of the critical titre below the images.

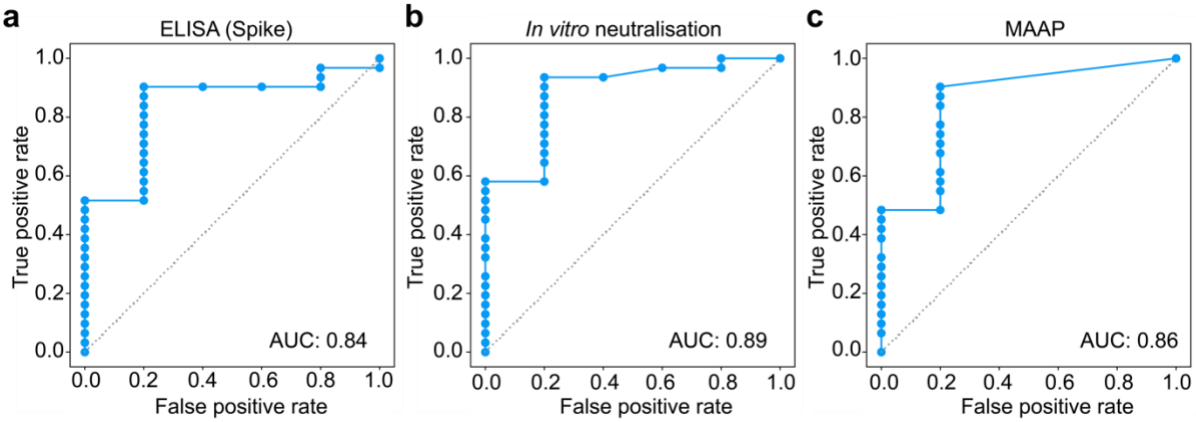

Figure S7: Receiver operating characteristic (ROC) curves demonstrating the ability of the ELISA EC_{50}(Spike) (a), *in vitro* ACE2 competition assay (b), and MAAP assay (c) to predict the ability of the serum to neutralise in the cytopathic-effect based neutralisation assay, regardless of titre.

Table S1. Demographic characterisation of the individuals used in our study.

Cohort	**Total number**	**Number male**	**Number female**	**Number undefined**	**Median age (IQR) - years**
Convalescent individuals	19	19	0	0	27 (22-49)
Healthy blood donors	20	8	10	2	31 (24-45)
Hospital patients	3	2	1	0	67 (65-74)

Table S2: Comparison of outcome on ACE2 competition and cytopathic-effect based assay, for all samples which were tested in the ACE2 competition, cytopathic-effect based assay, and had low enough background autofluorescence to be assessed by MAAP. Positive means that the radius has decreased compared to the ACE2-S1 complex. This is the aggregate statistics of the results presented in Fig. S7. A positive result in the ACE2 competition assay is here defined as yielding an effective R_h value smaller than 5.6 nm.

		Cytopathic-effect based neutralisation assay		
		Positive	Negative	Total
ACE2 competition	Positive	29	1	30
	Negative	2	4	6
	Total	31	5	36

Table S3: Comparison of outcome on ACE2 competition and cytopathic-effect based neutralisation assay. Here, we show the hydrodynamic radius based on the ACE2 competition assay as well as the titre of the neutralisation assay. Sera which did not neutralise in the cell plaque assay at any of the titres tested are indicated by 'none', whereas those that were not tested are indicated by 'N/A'.

Patient ID	**ACE2 competition assay R_h /nm**	**Critical titre for the cytopathic-effect based neutralisation assay (fraction)**
1	4.83	0.0125
2	4.98	0.0125
3	4.86	0.0125
4	5.36	0.003125
5	4.84	0.0125
6	4.79	0.05
7	4.82	0.05
8	4.62	0.05
9	N/A	0.003125
10	5.14	0.0125
11	5.11	0.0125
12	4.98	0.003125
13	5.18	0.05
14	NA	0.05
15	5.06	0.05
16	5.25	0.05
17	5.76	none
18	5.16	0.05
19	5.91	none
20	5.64	none
21	5.67	0.05
22	4.74	0.05
23	5.14	0.05
24	N/A	0.05
25	5.79	0.0125
26	4.84	0.05
27	5.41	0.0125
28	5.07	0.05
29	4.77	0.003125
30	5.35	0.05
31	5.26	0.05
32	4.81	0.05
33	4.72	0.05
34	5.67	none
35	4.96	0.0125
36	5.51	0.05
37	5.12	none
38	N/A	none
39	5.30	0.0125
40	5.08	0.05

References

1. Emmenegger, M. *et al.* Early peak and rapid decline of SARS-CoV-2 seroprevalence in a Swiss metropolitan region. *medRxiv* 2020.05.31.20118554 (2020) doi:10.1101/2020.05.31.20118554.
2. Gelman, A. *et al. Bayesian Data Analysis*. (Chapman and Hall/CRC, 2013).